Available online at www.sciencedirect.com
SCIENCE DIRECT®
Biochemical and Biophysical Research Communications 324 (2004) 212–217
BBRC
www.elsevier.com/locate/ybbrc

Amantadine partition and localization in phospholipid membrane: a solution NMR study

Junfeng Wang, Jason R. Schnell, James J. Chou*

Department of Biological Chemistry and Molecular Pharmacology, Harvard Medical School, 240 Longwood Avenue, Boston, MA 02115, United States

Received 25 August 2004
Available online 25 September 2004

Abstract

Quantification of membrane partition potential of drug compounds is of great pharmaceutical interest. Here, a novel approach combining liquid-state NMR diffusion measurements and fast-tumbling lipid/detergent bicelles is used to measure accurately the partition coefficient K_p of amantadine in phospholipid bilayers. Amantadine is found to have a strong membrane partition potential, with K_p of 27.6 in DMPC and 37.8 in POPC lipids. Electrostatic interaction also plays a major role in the drug's affinity towards biological membrane as introduction of negatively charged POPG dramatically increases its K_p. Saturation transfer difference experiments in small bicelles indicate that amantadine localizes near the negatively charged phosphate group and the hydrocarbon chain of bilayer lipid. The approach undertaken in this study is generally applicable for characterizing interactions between small molecules and phospholipid membranes.

Keywords: Amantadine; DHPC; POPC; Membrane partition; Fast-tumbling bicelle; Diffusion; NMR

Amantadine (1-aminoadamantane) is a licensed drug for treatment of influenza A viral infection [1]. It inhibits viral replication by blocking the channel activity of the M2 proton channel that is critical in the virus life cycle [2]. The mechanism of M2 channel inhibition remains a matter of debate. It is commonly thought that the drug inhibits proton conductance by plugging the N-terminal opening of the channel because amantadine-resistant mutations are mostly pore-lining residues near the N-terminal end of the channel [3,4]. However, the issue was made more complicated by the finding that the concentration of drug required for half-maximal inhibition of current is greater when the channel is open than in the closed state [5]. Moreover, amantadine readily partitions into lipid bilayers [6]. Taken together, the evidence suggests that amantadine may attack the membrane side of the channel, in contrast to the cork plugging the bottle model [7]. Therefore, an understanding of the partition properties of amantadine in membrane bilayers is needed to understand the drug–channel interactions.

Association between amantadine and cellular membrane was first illustrated in a study which demonstrated that the compound has a tendency to inhibit membrane fusion [6]. Neutron and X-ray diffraction studies then showed that while a majority of the drug occupies the head-group site of 1,2-dioleoyl-*sn*-glycero-3-phosphocholine (DOPC) close to the surface of membrane, some penetrate deep in the bilayer [8]. The partition potential of amantadine in membrane has also been examined indirectly by an EPR study, which measured the partition coefficient of a spin-labeled amantadine analog in DMPC vesicles to be 11.2 at 45 °C [9]. It was also shown in the EPR study that at least part of the spin-labeled amantadine is deeply buried in the hydrocarbon chain region of the membrane.

* Corresponding author. Fax: +1 617 432 2921.
E-mail address: james_chou@hms.harvard.edu (J.J. Chou).

0006-291X/$ - see front matter © 2004 Elsevier Inc. All rights reserved.
doi:10.1016/j.bbrc.2004.09.039

This report describes a novel use of liquid-state NMR techniques and fast-tumbling bicelles, or bilayered micelles, for the accurate measurement of amantadine partition coefficient in phospholipid bilayers. Concomitantly, the site of interaction between the drug and the phospholipid bilayer of DMPC/DHPC bicelles is observed by saturation transfer difference NMR spectroscopy [10]. The approaches described here are generally applicable for rapid and detailed characterization of drug–membrane interactions.

Materials and methods

1,2-Dicaproyl-*sn*-glycero-3-phosphocholine (DHPC), 1,2-dimyristoyl-*sn*-glycero-3-phosphocholine (DMPC), 1-palmitoyl-2-oleoyl-*sn*-glycero-3-phosphocholine (POPC), 1-palmitoyl-2-oleoyl-*sn*-glycero-3-[phospho-rac-(1-glycerol)] (POPG), and CHAPSO were purchased from Avanti Polar Lipids and used as received. Perdeuterated DHPC was purchased from Cambridge Isotope Laboratories. 1-Aminoadamantane was obtained from Sigma.

Sample preparation. All micelle and bicelle samples were prepared in 20 mM phosphate buffer, pH 7.2, 90% H_2O, 10% D_2O, and 1 mM azide. Bicelle samples were made by first preparing a concentrated stock solution of DHPC (400 mM) in buffer. Then an appropriate amount of this stock solution was added to a weighed amount of lipid (in powder form), followed by thorough mixing until all lipids were dissolved and the solution was completely clear. The molar ratio, q, of lipid versus bicelle-bound DHPC was kept at 0.3 for all diffusion measurements. Here, the concentration of free DHPC in the presence of small bicelles was assumed to be 7 mM [11]. For the POPC/POPG/DHPC bicelle sample, a molar ratio of the zwitterionic POPC to the negatively charged POPG was 1:1. For measuring diffusion rates of drug in the presence of bicelles or micelles, a 0.5 M amantadine stock solution (in H_2O) was added to a lipid/detergent solution, and the final pH confirmed with a micro pH electrode (VWR). For saturation transfer difference (STD) experiments, a $q = 1$ DMPC/[^{2}H]DHPC was made as above with total weight fraction of surfactant being 0.1.

In order to restrict the sample volume to the region over which the field gradients are most linear and to minimize the effects of temperature gradients, all experiments were carried out in Shigemi microcells (Shigemi, Allison Park, PA), with the sample length adjusted to 12 mm.

NMR measurement of diffusion rates. NMR diffusion experiments were performed on a Bruker DMX-600 NMR spectrometer operating at a ^{1}H frequency of 600 MHz, containing a cryoprobe with self-shielded pulsed field gradients in the z direction. All diffusion rates used for deriving partition coefficients were measured at 25 °C and ambient pressure. The gradients were calibrated at 25 °C on the residual ^{1}H signal in a sample of 99.9% D_2O, using the published value of $1.902 \pm 0.002 \times 10^{-9}$ m^2 s^{-1} for the self-diffusion coefficient of HDO at 25 °C [12–14]. The gradient strengths were found to be 54.7 G/cm at the maximum current for the z gradient coils. The sample temperature was calibrated by directly placing a thermocouple probe inside a Shigemi microcell at the center of the sample. All diffusion measurements were carried out using the BPP-LED experiment shown in Fig. 1A [11,15]. While fixing the gradient duration δ, the diffusion delay T, and τ, the strength of the two pairs of bipolar square gradients (G1) was increased stepwise in the z direction. For measurements of small compounds that diffuse faster than 10×10^{-11} m^2 s^{-1}, $\delta = 3.0$ ms, $\tau = 1.0$ ms, and $T = 50$ ms, whereas for slower diffusing micelles and bicelles, $\delta = 4.0$ ms, $\tau = 0.5$ ms, and $T = 200$ ms.

The translational self-diffusion coefficient D_S is obtained from the least-squares linear fit of

$$\ln[I(f)/I(f_0)] = -(\gamma\delta G_{max})^2(f^2 - f_0^2)(\Delta - \delta/3 - \tau/2)D_S, \quad (1)$$

where $I(f)$ is the intensity of the NMR signal as a function of the fractional gradient strength, f is incremented from 0.05 to 0.50 in steps of 0.05, f_0 is the fractional gradient strength of the reference spectrum (0.05), γ is the gyromagnetic ratio of ^{1}H, and G_{max} is the maximum gradient strength (54.7 G/cm) offered by the z gradient coils at $f = 1$. The delays Δ, δ, and τ are defined in Fig. 1A. In order to minimize the effect of gradient non-linearity, all gradient decay curves (including that of the HDO reference measurement) were measured over a gradient range that caused a maximum attenuation by about a factor of 20.

Deriving K_p from translational diffusion coefficients. The partition coefficient (K_p), which quantifies drug lipophilicity, is defined as the ratio of drug concentration in membrane to its concentration in water, given the equal volume fraction of membrane and water. This definition is similar to that of the octanol/water partition coefficient (K_{ow}), which has been the subject of extensive literature (as described, e.g., in [16]) for estimating the lipophilicity of drug compounds. In the case of amantadine, where its lipid/H_2O partition is in fast exchange, chemical shift resonances of the drug associated with lipid and H_2O cannot be distinguished. Hence, D_S measured for amantadine in the presence of bicelles is a weighted average of the contributions from free and bicelle-associated molecules. Given two relevant states of the molecule, bicelle-associated and water-associated, their populations can be easily calculated from the relation

$$D_{AVG} = D_L F_L + D_F(1 - F_L), \quad (2)$$

where D_F and D_L denote the diffusion coefficients of free and lipid-associated drug, respectively, D_{AVG} is the average D_S of the drug measured in the presence of bicelles, and F_L is the molar fraction of drug bound to the bicelles. D_L must equal the bicelle diffusion coefficient

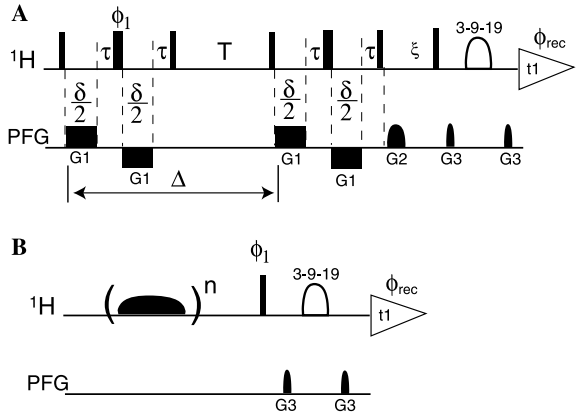

Fig. 1. Pulse schemes of the LED diffusion (A) and saturation transfer difference (B) experiments employed in this study. Narrow and wide pulses correspond to flip angles of 90° and 180°, respectively. All pulse phases are x, unless specified otherwise. In (A), the BPP-LED experiment [11,15] has the 3-9-19 water suppression element [26] for readout. For diffusion measurements of small compounds that diffuse faster than 10×10^{-11} m^2 s^{-1}, $\delta = 3.0$ ms, $\tau = 1.0$ ms, and $T = 50$ ms, whereas for slower diffusing micelles and bicelles, $\delta = 4.0$ ms, $\tau = 0.5$ ms, and $T = 200$ ms. The G1 rectangular pulsed field gradients are applied in the z direction, at variable strength (see text). G2 is sine-bell shaped with a peak amplitude of 25 G/cm, 1.2 ms in duration, applied along the z axis. In (B), the Gaussian pulse used for selective resonance saturation is 50 ms in length and 125 Hz in power; it is repeated n times (see text) with 1 ms interval. In both (A) and (B), the Watergate gradient G3 is sine-bell shaped, with a peak amplitude of 27 G/cm, 1.0 ms in duration and applied along the z axis. Phase cycling: (a) $\phi_1 = x, y, -x, -y$ and $\phi_{rec} = x, -x$; (b) $\phi_1 = x, -x$ and $\phi_{rec} = x, -x$.

(D_B). For DMPC/DHPC bicelles, D_B was obtained using the non-overlapping DMPC ^{1}H resonance at 0.84 ppm, whereas for POPC/DHPC or POPC/POPG/DHPC bicelles, the distinct POPC resonance at 2.00 ppm was used. D_F was obtained from the diffusion coefficient of amantadine in the absence of solute obstruction (D_f), measured with 1 mM amantadine dissolved in 90% H_2O, 10% D_2O, and using the ^{1}H resonance at 1.91 ppm. The effect of obstruction from bicelles in the drug–bicelle mixture was calculated using the relation [17]:

$$D_F = D_f/(1 + \phi/2), \quad (3)$$

where ϕ is the hydrodynamic volume fraction of the bicelles which is approximated here by the weight fraction of phospholipids (excluding 7 mM monomer DHPC). Having experimentally measured D_{AVG}, D_B, and D_f, F_L was calculated from Eqs. (2) and (3). The partition coefficient of the drug for bicelles, K_p^A, is therefore

$$K_p^A = [F_L/(1 - F_L)](1 - \phi)/\phi. \quad (4)$$

The partition coefficient given by Eq. (4) is attributed to both lipid and detergent within the bicelles. If the partition coefficient for detergent micelles (K_p^D) is known, then the partition coefficient for the lipid bilayer region of the bicelles (K_p^L) can be derived from the relation

$$K_p^A = V_L K_p^L + V_D K_p^D, \quad (5)$$

where V_L and V_D represent volume fractions of lipid and detergent in bicelles, respectively, satisfying the relation $V_L + V_D = 1$.

Saturation transfer difference experiment. The STD experiments were performed on a Bruker DRX-750 NMR spectrometer operating at a ^{1}H frequency of 750 MHz, containing a TXI triple-resonance (^{1}H, ^{13}C, and ^{15}N) probehead with self-shielded pulsed field gradients in the z direction. To observe steady-state NOE transfer between drug and lipid, a $q = 1.0$ bicelle sample containing 43 mM perdeuterated DHPC (D40-DHPC), 43 mM regular DMPC, 5 mM amantadine, and 99.9% D_2O was used. DMPC ^{1}H resonances at 4.03, 3.25, 1.29, and 0.84 ppm, corresponding to the glycerol methylene, choline methylene, hydrocarbon chain methylene, and hydrocarbon chain terminal methyl group, respectively, were selectively saturated with a train of 50 ms Gaussian pulses separated by 1 ms. The changes in the intensity of amantadine resonance (1.91 ppm) were recorded at saturation times of 0.25, 0.75, 1, 1.5, 2, 2.5, and 5 s.

Results

The partition coefficient of amantadine in DHPC micelles was determined for a sample containing 221 mM DHPC and 5 mM amantadine in 20 mM phosphate buffer, pH 7.2, 90% H_2O, and 10% D_2O. The average D_S of the drug (D_{AVG} in Eq. (2)) was measured to be 29.3×10^{-11} m^2 s^{-1}. D_S of free amantadine in the absence of obstruction in a 1 mM amantadine sample was measured to be 72.2×10^{-11} m^2 s^{-1}. In the presence of obstruction from DHPC micelles (~10% of sample volume taking DHPC density and hydration into account), D_F in Eq. (2) becomes 68.8×10^{-11} m^2 s^{-1} according to Eq. (3). The diffusion coefficient of drug partitioned into micelles, or D_L in Eq. (2), is equal to D_S of the micelle-associated DHPC molecules. Due to the fact that chemical shift resonances of micelle-associated and monomeric DHPC cannot be resolved even at very high spectral resolution, it was only possible to measure their average diffusion rate. However, since D_S of monomeric DHPC in water in the absence of obstruction was previously determined to be 43.8×10^{-11} m^2 s^{-1} at 27 °C [11], and measured here using a 5 mM DHPC sample at 25 °C to be $43.5 \pm 1 \times 10^{-11}$ m^2 s^{-1}, D_S of monomeric DHPC in the presence of micelle obstruction can be scaled according to Eq. (3). Knowing the average D_S (9.30×10^{-11} m^2 s^{-1}), D_S of monomeric DHPC in the sample (41.4×10^{-11} m^2 s^{-1}), concentration of monomeric DHPC (14 mM) [11,18], and total concentration of DHPC in the sample (221 mM), D_S of the micelle-bound DHPC (or equivalently D_S of the micelles) was found to be 7.13×10^{-11} m^2 s^{-1}. Finally, by combining Eqs. (2) and (4), K_p^A of amantadine in a DHPC/H_2O binary system was found to be 16.0.

For the sample containing 22 mM POPC, 22 mM POPG, 146 mM DHPC, and 5 mM amantadine, D_{AVG} of the drug was found to be 17.1×10^{-11} m^2 s^{-1}. Since the concentration of monomeric lipid is zero in water, amantadine partitioned into bicelles must diffuse at the same rate as the lipids. Hence, D_L in Eq. (2) was measured, using the non-overlapping POPC resonance at 2.00 ppm, to be 5.46×10^{-11} m^2 s^{-1}. Similar to the case

Table 1
Diffusion constants and derived amantadine partition coefficients for various detergents and lipids

Sample[a]	D_{AVG} (10^{-11} m^2 s^{-1})[b]	D_B (10^{-11} m^2 s^{-1})[c]	K_p^A	K_p^L
DHPC	29.3 ± 0.4	7.13[d] ± 0.08	16.0 ± 0.2	
DMPC/DHPC	25.8 ± 0.4	6.21 ± 0.08	19.7 ± 0.3	27.6 ± 0.6
POPC/DHPC	23.2 ± 0.3	5.90 ± 0.07	23.7 ± 0.5	37.8 ± 0.4
POPC/POPG/DHPC	17.1 ± 0.2	5.46[e] ± 0.07	39.9 ± 0.5	84.0 ± 1.1
CHAPSO	27.5 ± 0.4	7.56[f] ± 0.09	18.6 ± 0.3	
DMPC/CHAPSO	24.8 ± 0.4	7.32 ± 0.08	22.7 ± 0.3	27.3 ± 0.7

[a] All samples contain 5 mM amantadine, 10% w/w surfactants, and lipid/detergent ratios of 0.3.
[b] The average diffusion rate of amantadine in micelle or bicelle solutions.
[c] D_S of micelle or bicelle at a surfactant volume fraction of ~0.1. Note that these are not the true self-diffusion rates in the absence of obstruction.
[d] D_S of micelle-bound DHPC, calculated using a DHPC critical micelle concentration of 14 mM, total DHPC concentration of 221 mM, and average observed DHPC D_S of 9.30×10^{-11} m^2 s^{-1}.
[e] The molar ratio of POPC:POPG is 1:1.
[f] D_S of micelle-bound CHAPSO, calculated using a CHAPSO critical micelle concentration of 8 mM, total CHAPSO concentration of 159 mM, and average observed CHAPSO D_S of 8.987×10^{-11} m^2 s^{-1}.

of the drug–micelle mixture, D_F in Eq. (2) was found to be 68.8×10^{-11} m^2 s^{-1}. Using the values of D_L, D_F, and bicelle volume fraction of 0.1, the drug K_p^A for $q = 0.3$ POPC/POPG/DHPC bicelles is 39.9. Since we already know the K_p for DHPC micelles and the approximate volume fraction of DHPC in the bicelles, the K_p^L for POPC/POPG bilayer is derived from Eq. (5) to be 84.0. Table 1 lists the K_p of amantadine in DHPC and CHAPSO micelles and various types of bicelles including DMPC/DHPC, POPC/DHPC, POPC/POPG/DHPC, and DMPC/CHAPSO.

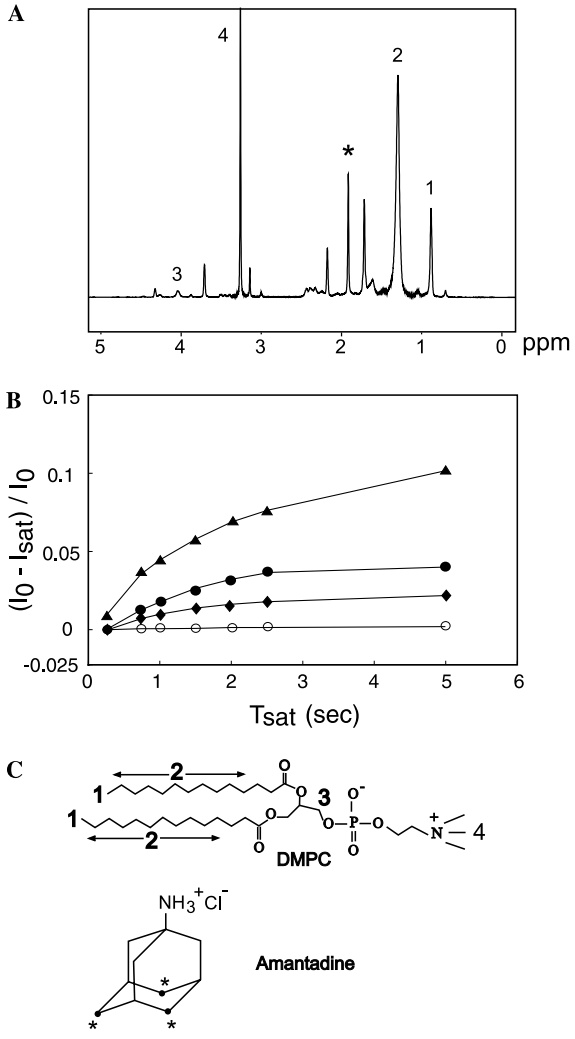

Fig. 2. Localization of amantadine in the DMPC bilayer region of the $q = 1.0$ DMPC/D40-DHPC bicelles by STD experiments. (A) 1D ^{1}H spectrum of $q = 1.0$ DMPC/D40-DHPC bicelle sample containing 5 mM amantadine acquired at ^{1}H frequency of 750 MHz. Four DMPC resonances (numbered in (A) and (C)) were selectively saturated: the terminal methyl group of myristic acid hydrocarbon chain (peak 1 at 0.84 ppm), the methylene groups of the hydrocarbon chain (peak 2 at 1.29 ppm), glycerol methylene (peak 3 at 4.03 ppm), and choline methylene (peak 4 at 3.25 ppm). The NOE transfer is monitored by the amantadine signal at 1.91 ppm (marked with * in (A) and (C)). The saturated intensity, I_{sat}, is compared with the reference intensity, I_0, obtained from a spectrum taken with off-resonance excitation at 14 ppm. (B) The observed STD effects, $(I_0 - I_{sat})/I_0$, with saturation at various DMPC resonances were plotted against the saturation time, T_{sat}. The symbols represent: (▲) chain methylene; (●) chain methyl; (♦) glycerol methylene; and (○) choline methyl. (C) Chemical drawings of amantadine and DMPC; the drug–lipid interaction sites are labeled with numbers in bold face.

In STD experiments, the steady-state NOE transfers between drug and lipid protons were measured by selectively saturating the individual non-overlapping DMPC resonances at 4.03, 3.25, 1.29, and 0.84 ppm (see Fig. 2A). The consequent NOE contribution is measured as a decrease in the amantadine resonance intensity at 1.91 ppm. Due to spin diffusion in the lipid, longer saturation times yield larger decreases in the amantadine resonance intensity. For example, when irradiating the methylene resonances of the hydrocarbon chain at 1.29 ppm, where spin diffusion can be the greatest, the NOE transfer builds up rapidly and approaches equilibrium after 3 s of saturation. At this point, the amantadine peak intensity decreases by as much as 10%. Fig. 2B shows the NOE buildup curves corresponding to the saturation of different ^{1}H resonances of DMPC.

Discussion

Therapeutically useful drugs must cross several hydrophilic and lipophilic barriers in order to reach their target [19]. In many instances, the drug must be soluble in both the cytosol and membrane. Therefore, a thorough characterization of the partitioning of small molecules into membrane bilayers is of paramount importance in drug development.

Liquid-state NMR spectroscopy is an effective tool for providing high-resolution information on the structure and dynamics of biological compounds under near-native conditions. In the current study, solution NMR was applied to investigate small-molecule interactions with phospholipid bilayers through the use of fast-tumbling bicelles. Thus, it is important to first establish that the lipid/detergent mixtures can adequately model true lipid bilayers.

When DMPC and DHPC are mixed in water, they aggregate to form bilayered micelles containing a small patch of lipid bilayer that is morphologically similar to a true lipid bilayer, surrounded by an annulus of detergent [11,20–23]. Recently, in a separate study, we made an interesting observation that the lipids in small DMPC/DHPC bicelles ($q > 0.3$) also exhibit the gel-to-fluid phase transition characteristic of lipid bilayers. In this case the melting transition temperature is 21 °C for a $q = 1$ bicelle, very close to the DMPC melting temperature of 23 °C in extended lipid bilayers (data not shown). To confirm that the detergent rim does not have a large effect on the drug–lipid interaction, the K_p^L of amantadine in a DMPC bilayer obtained using the

DMPC/DHPC bicelles was cross-validated by repeating the measurement using DMPC/CHAPSO bicelles.

For the $q = 0.3$ DHPC/CHAPSO bicelle sample containing 5 mM amantadine, D_{AVG} of the drug was determined to be 24.8×10^{-11} m^2 s^{-1}, and D_L from DMPC resonance was 7.32×10^{-11} m^2 s^{-1}. K_p^A, the partition coefficient of amantadine in bicelle, is then calculated to be 22.7. As exemplified for the DHPC/POPC/POPG bicelle, K_p^A has contributions from drug molecules in both the DMPC bilayer and the CHAPSO rim. The K_p in the CHAPSO rim, which is assumed to be the same as in the CHAPSO micelle environment, was measured to be 18.6 for a CHAPSO/amantadine sample according to steps described above for measuring amantadine K_p in DHPC micelles, and assuming a CHAPSO critical micelle concentration of 8 mM [24]. Using Eq. (5), the K_p^L of amantadine in DMPC bilayer was determined to be 27.3, in excellent agreement with the value (27.6) derived from the $q = 0.3$ DMPC/DHPC bicelle (Table 1). Hence, by employing the correction strategy described in Eq. (5) and subtracting the effects of detergent–drug interaction, a highly reliable K_p^L can be obtained using the small bicelles.

The partition coefficients of amantadine in bicelle/H_2O binary systems (shown in Table 1) indicate a strong partition potential of the drug in phospholipid membrane. For DMPC, the K_p^L derived from DMPC/DHPC and DMPC/CHAPSO bicelles is 27.5 ± 0.6, meaning that the probability of amantadine residing in the lipid bilayer is greater than 96%, given equal volume of lipid and water. The results indicate that amantadine preferentially resides in the lipid bilayer, and also suggests that the drug would easily pass through cellular membranes. In a previous EPR study using a spin-labeled derivative of amantadine, K_p^L in DMPC vesicle was found to be 11.2 at 45 °C, more than a factor of 2 lower than that of the parent amantadine compound. As previously suggested by Subczynski et al. [9], the difference is probably due to the fact that amantadine is more hydrophobic than its nitroxide-linked derivative. When 50% of zwitterionic POPC in the $q = 0.3$ bicelles is replaced with negatively charged POPG, K_p^L almost doubled (Table 1), suggesting that at physiological pH, electrostatic interactions are an important factor in amantadine's lipophilicity.

Based on K_p^L shown in Table 1, the dissociation constant for amantadine–DMPC interaction is estimated to be roughly 10^{-2} M. Owing to the low affinity, only very weak NOEs were observed between drug and DMPC in a 2D ^{1}H NOESY spectrum recorded with 400 ms mixing time. Similar difficulty was encountered in the ROESY experiment (data not shown). To better examine interactions between drug and lipid, the STD experiments, which are much more effective in detecting weak bindings [10], were performed. Not surprisingly, there is no NOE contribution from the highly mobile $N(CH_3)_3$ group of DMPC, indicating that the drug does not reside on the surface of phospholipid bilayer. This was also shown by neutron diffraction studies of amantadine in DOPC bilayers [8]. Excitation of the other three DMPC resonances marked in Fig. 2A resulted in saturation transfer to amantadine (Fig. 2B). The initial NOE transfer rate is highest for the methylene protons in the hydrocarbon chain. However, this is likely due to spin diffusion along the proton-dense hydrocarbon chain. The initial buildup rates for the glycerol methylene and the terminal methyl groups are very similar. It is emphasized here that due to the uneven distribution of lipid protons and overlapping methylene resonances (shown in Fig. 2A), the distribution of amantadine in the bilayer cannot be quantified. However, qualitatively, the STD results indicate that the drug distribution spans the bilayer region encompassing the glycerol CH_2 near the negatively charged phosphate group and the entire hydrocarbon chain. This observation is consistent with previous neutron diffraction and EPR studies [8,9].

Another interesting observation is that amantadine ^{1}H linewidth in both DMPC/DHPC and POPC/DHPC bicelle is 6.6 Hz, not very different from that in water (6.1 Hz), after being normalized to account for the relative population of drug in lipid. This confirms the observation from NOESY experiments that the drug does not bind strongly to lipid and is therefore expected to tumble freely and diffuse laterally in the bilayer. Such a property may be of interest when designing drugs to target membrane proteins, because a search on a hypersurface is much more efficient than in a 3D space. One may envision a design scheme that uses organelle-specific lipid composition for the initial recruitment of drugs, and then allow the drugs to find the target protein efficiently by restricting the search to a two-dimensional random walk on the cellular membrane hypersurface. Results obtained in the current study allude to such a property of amantadine.

In conclusion, it is confirmed that amantadine is significantly more soluble in lipid bilayers than in aqueous solution, with amantadine preferring DMPC and POPC bilayers over aqueous solution by 2.0 and 2.2 kcal/mol, respectively. This is consistent with the role of amantadine in inhibiting the viral ion channel M2, as well as its effects on membrane fusion.

Furthermore, the current study suggests that small bicelles made from lipid/detergent mixtures can serve as a good model system of extended lipid bilayers. The fast-tumbling nature of the small bicelles allows solution-state NMR studies to be carried out on lipid bilayers and their interactions with small molecules as demonstrated in this study, as well as with biological macromolecules such as proteins and carbohydrates. As has been pointed out [25], the lipid composition of small bicelles can be tailored to reflect those that occur in natural membranes. As noted with amantadine in the

presence of POPC and POPC/POPG mixed bicelles, the exact lipid composition can have large effects on the energetics of interaction. Solution NMR experiments can provide quantitative and site-specific information on these interactions.

Acknowledgments

This study is supported by the Smith Family Award for Young Investigators and the PEW Scholarship.

References

[1] J.S. Oxford, A. Galbraith, Antiviral activity of amantadine: a review of laboratory and clinical data, Pharmacol. Ther. 11 (1980) 181–262.
[2] L.H. Pinto, L.J. Holsinger, R.A. Lamb, Influenza virus M2 protein has ion channel activity, Cell 69 (1992) 517–528.
[3] A.J. Hay, A.J. Wolstenholme, J.J. Skehel, M.H. Smith, The molecular basis of the specific anti-influenza action of amantadine, EMBO J. 4 (1985) 3021–3024.
[4] P. Astrahan, I. Kass, M.A. Cooper, I.T. Arkin, A novel method of resistance for influenza against a channel-blocking antiviral drug, Proteins: Struct. Funct. Bioinf. 55 (2004) 251–257.
[5] C. Wang, K. Takeuchi, L.H. Pinto, R.A. Lamb, Ion channel activity of influenza A virus M2 protein: characterization of the amantadine block., J. Virol. 67 (1993) 5585–5594.
[6] R.M. Epand, R.F. Epand, R.C. McKenzie, Effects of viral chemotherapeutic agents on membrane properties. Studies of cyclosporin A, benzyloxycarbonyl-D-Phe-L-Phe-Gly and amantadine, J. Biol. Chem. 262 (1987) 1526–1529.
[7] L.H. Pinto, R.A. Lamb, Understanding the mechanism of action of the anti-influenza virus drug amantadine., Trends Microbiol. 3 (1995) 271.
[8] K.C. Duff, A.J. Cudmore, J.P. Bradshaw, The location of amantadine hydrochloride and free base within phospholipid multilayers: a neutron and X-ray diffraction study, Biochim. Biophys. Acta (1993) 149–156.
[9] W.K. Subczynski, J. Wojas, V. Pezeshk, A. Pezeshk, Partitioning and localization of spin-labeled amantadine in lipid bilayers: an EPR study, J. Pharm. Sci. 87 (1998) 1249–1254.
[10] M. Mayer, B. Meyer, Characterization of ligand binding by saturation transfer difference NMR spectroscopy, Angew. Chem. Int. Ed. 38 (1999) 1784–1788.
[11] J.J. Chou, J.L. Baber, A. Bax, Characterization of phospholipids mixed micelles by translational diffusion, J. Biomol. NMR 29 (2004) 299–308.
[12] R. Mills, Self-diffusion in normal and heavy water in the range 1–45°, J. Phys. Chem. 77 (1973) 685–688.
[13] M. Holz, H. Weingartner, Calibration in accurate spin-echo self-diffusion measurements using H-1 and less-common nuclei, J. Magn. Reson. 92 (1991) 115–125.
[14] W.S. Price, W.S. Price, Pulsed-field gradient nuclear magnetic resonance as a tool for studying translational diffusion. 1. Basic theory, Concepts Magn. Reson. 9 (1997) 299–336.
[15] D.H. Wu, A.D. Chen, C.S. Johnson, An improved diffusion-ordered spectroscopy experiment incorporating bipolar-gradient pulses, J. Magn. Reson. A 115 (1995) 260–264.
[16] J. Sangster, Octanol–Water Partition Coefficients: Fundamentals and Physical Chemistry, Wiley, New York, 1997.
[17] H. Johannesson, B. Halle, Solvent diffusion in ordered macrofluids: a stochastic simulation study of the obstruction effect, J. Chem. Phys. 104 (1996) 6807–6817.
[18] R.A. Burns, M.F. Roberts, R. Dluhy, R. Mendelsohn, Monomer-to-micelle transition of dihexanoylphosphatidylcholine: carbon-13 NMR and Raman studies, J. Am. Chem. Soc. 104 (1982) 430–438.
[19] R. Mannhold, H. Kubinyi, G. Folkers, J.K. Seydel, M. Wiese, Drug–Membrane Interactions: Analysis, Drug Distribution, Modelling, Wiley, New York, 2000.
[20] C.R. Sanders, R.S. Prosser, Bicelles: a model membrane system for all seasons? Structure Fold. Des. 6 (1998) 1227–1234.
[21] J.J. Chou, J.D. Kaufman, S.J. Stahl, P.T. Wingfield, A. Bax, Micelle-induced curvature in a water-insoluble HIV-1 Env peptide revealed by NMR dipolar coupling measurement in stretched polyacrylamide gel, J. Am. Chem. Soc. 124 (2002) 2450–2451.
[22] S. Gaemers, A. Bax, Morphology of three lyotropic liquid crystalline biological NMR media studied by translational diffusion anisotropy, J. Am. Chem. Soc. 123 (2001) 12343–12352.
[23] K.J. Glover, J.A. Whiles, G. Wu, N. Yu, R. Deems, J.O. Struppe, R.E. Stark, E.A. Komives, R.R. Vold, Structural evaluation of phospholipid bicelles for solution-state studies of membrane-associated biomolecules, Biophys. J. 81 (2001) 2163–2171.
[24] L.M. Hjelmeland, D.W. Nebert, J.C. Osborne, Sulfobetaine derivatives of bile-acids—non-denaturing surfactants for membrane biochemistry, Anal. Biochem. 130 (1983) 72–82.
[25] R.R. Vold, R.S. Prosser, A.J. Deese, Isotropic solutions of phospholipid bicelles: a new membrane mimetic for high-resolution NMR studies of polypeptides, J. Biomol. NMR 9 (1997) 329–335.
[26] V. Sklenar, M. Piotto, R. Leppik, V. Saudek, Gradient-tailored water suppression for ^{1}H–^{15}N HSQC experiments optimized to retain full sensitivity, J. Magn. Reson. A 102 (1993) 241–245.